Cancellation of Multiuser Interference due to Carrier Frequency Offsets in Uplink OFDMA

S. Manohar, V. Tikiya, D. Sreedhar, and A. Chockalingam
Department of ECE, Indian Institute of Science, Bangalore 560012, INDIA

***Abstract*— In uplink orthogonal frequency division multiple access (OFDMA) systems, multiuser interference (MUI) occurs due to different carrier frequency offsets (CFO) of different users at the receiver. In this paper, we present a multistage linear parallel interference cancellation (LPIC) approach to mitigate the effect of this MUI in uplink OFDMA. The proposed scheme first performs CFO compensation (in time domain) followed by K DFT operations (where K is the number of users) and multistage LPIC on these DFT outputs. We present a detailed performance and complexity comparison of the proposed scheme with another scheme proposed recently by Huang and Letaief which performs CFO compensation and interference cancellation in frequency domain using Circular Convolution (we refer to this scheme as HLCC scheme). We show that the HLCC scheme performs better than our scheme when the individual CFO values are small, whereas our scheme performs better than the HLCC scheme when the CFO differences are small (even if the individual CFO values are large). Also, our scheme has lesser complexity than HLCC scheme when the number of subcarriers is large, which is typical in OFDMA systems.**

Keywords *– Uplink OFDMA, carrier frequency offset, multiuser interference, interference cancellation.*

I. Introduction

Recently, there has been increased research focus on orthogonal frequency multiple access (OFDMA) on the *uplink* [1]-[11]. In OFDM/OFDMA systems, carrier frequency offset (CFO) between transmit and receive carrier frequencies results in loss of orthogonality among different subcarriers at the receiver. In uplink OFDMA, correction to one user's CFO would misalign other users. Thus, other user CFO will result in multiuser interference (MUI) in uplink OFDMA. There have been few recent attempts that address the issue of MUI due to other user CFO in uplink OFDMA [7]-[11]. Interference cancellation (IC) techniques can be employed at the base station receiver to mitigate the MUI effects [8]-[11]. Recently, in [9], Huang and Letaief presented an IC approach which performs CFO compensation and MUI cancellation in frequency domain using circular convolution. We refer to this scheme in [9] as **H**uang-**L**etaief **C**ircular **C**onvolution (HLCC) scheme. The circular convolution approach was proposed earlier by Choi et al in [6] as an alternative to the direct time-domain method of CFO compensation. Huang and Letaief refer the scheme in [6] as CLJL scheme (CLJL stands for the first letters of the names of the four authors of [6]). The CLJL scheme does not perform MUI cancellation. The HLCC scheme, on the other hand, uses circular convolution for both CFO compensation (as in [6]) as well as MUI cancellation. More recently, in [10], we proposed a minimum mean square error (MMSE) receiver for MUI cancellation in uplink OFDMA. We derived a recursion to approach the MMSE solution and showed that this recursive MMSE solution encompasses the CLJL and HLCC schemes as special cases.

Structure-wise, a common feature in CLJL [6], HLCC [9], and MMSE [10] schemes is that all these detectors/cancellers first perform a single DFT operation on the received samples and the resulting DFT output vector is further processed to achieve CFO compensation and MUI cancellation using circular convolution. Here, we propose and analyze an alternate MUI cancellation receiver structure which first performs CFO compensation in time domain, followed by K DFT operations (where K is the number of users) and multistage linear parallel interference cancellation (LPIC) on these DFT outputs. We scale the estimated MUI by weights before cancellation. We obtain closed-form expressions for the optimum weights that maximize the average signal-to-interference ratio (SIR) at the output of the different LPIC stages.

Comparing the proposed weighted LPIC (WLPIC) scheme with the HLCC scheme in [9], we show that i) in terms of complexity, the proposed WLPIC scheme is less complex than the HLCC scheme, particularly when the number of subcarriers is large (which is typical in OFDMA systems), and ii) in terms of performance, while the bit error performance of the HLCC scheme is affected by the individual CFO values of all the users, the performance of the WLPIC scheme is affected by the difference between the desired user's and other users' CFO values. Because of this, the HLCC scheme performs better than the WLPIC scheme when the individual CFO values are small, whereas the WLPIC scheme performs better than HLCC scheme when the CFO differences are small (even if the individual CFO values are large).

II. Uplink OFDMA System Model

We consider an uplink OFDMA system with K users, where each user communicates with a base station through an independent multipath channel as shown in Fig. 1. We assume that there are N subcarriers in each OFDM symbol and one subcarrier can be allocated to only one user. The information symbol for the ith user on the kth subcarrier is denoted by $X_k^{(i)}$, $k \in S_i$, where S_i is the set of subcarriers assigned to user i and $E\left[\left|X_k^{(i)}\right|^2\right] = 1$. Then, $\bigcup_{i=1}^{K} S_i = \{0, 1, \ldots, N-1\}$ and $S_i \bigcap S_j = \phi$, for $i \neq j$. The length of the guard interval added is N_g samples and is assumed to be longer than the maximum channel delay spread. After IDFT processing and guard interval insertion at the transmitter, the time domain sequence of the ith user, $x_n^{(i)}$, is given by

$$x_n^{(i)} = \frac{1}{N} \sum_{k \in S_i} X_k^{(i)} e^{\frac{j2\pi nk}{N}}, \quad -N_g \leq n \leq N-1. \quad (1)$$

This work was supported in part by the Swarnajayanti Fellowship, Department of Science and Technology, New Delhi, Government of India, under Project Ref: No. 6/3/2002-S.F.

1-4244-0355-3/06/$20.00 (c) 2006 IEEE

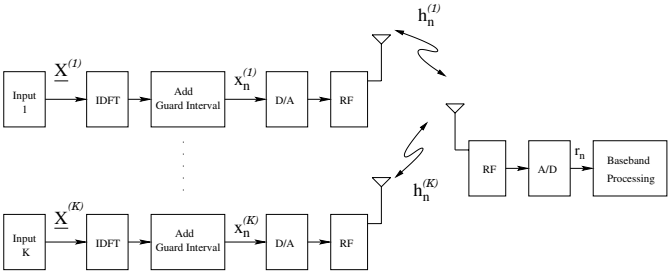

Fig. 1. Uplink OFDMA system model.

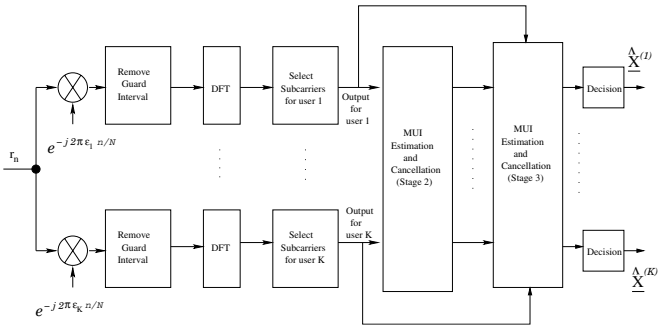

Fig. 2. Receiver baseband processing – CFO compensation (in time domain) and interference cancellation.

The ith user's signal, after passing through the channel, is given by

$$s_n^{(i)} = x_n^{(i)} \star h_n^{(i)} \tag{2}$$

where $\star$ denotes linear convolution and $h_n^{(i)}$ is the ith user's channel impulse response. It is assumed that $h_n^{(i)}$ is non-zero only for $n = 0, \ldots, L-1$, where L is the maximum channel delay spread, and that all users' channels are statistically independent. We assume that $h_n^{(i)}$'s are i.i.d. complex Gaussian with zero mean and $E\Big[\Big(h_{n,I}^{(i)}\Big)^2\Big] = E\Big[\Big(h_{n,Q}^{(i)}\Big)^2\Big] = 1/L$, where $h_{n,I}^{(i)}$ and $h_{n,Q}^{(i)}$ are the real and imaginary parts of $h_n^{(i)}$. The channel coefficient in frequency domain $H_k^{(i)}$ is given by

$$H_k^{(i)} = \sum_{n=0}^{L-1} h_n^{(i)} e^{\frac{-j2\pi nk}{N}}, \tag{3}$$

and $E\Big[\Big|H_k^{(i)}\Big|^2\Big] = 2$. The received baseband signal after coarse carrier frequency tracking (leaving some residual carrier frequency offset) is given by

$$r_n = \sum_{i=1}^{K} s_n^{(i)} e^{\frac{j2\pi\epsilon_i n}{N}} + z_n, \quad -N_g \le n \le N-1, \tag{4}$$

where $\epsilon_i, i = 1, \ldots, K$ denotes the ith user's CFO normalized by the subcarrier spacing, and z_n is the AWGN with zero mean and variance σ^2. We assume that all users are time synchronized and that $\epsilon_i, i = 1, \cdots, K$ are known at the receiver.

Figure 2 shows the receiver baseband processing including i) CFO compensation in time domain and guard time removal, ii) K DFT operations (one for each user), and iii) linear parallel interference cancellation (LPIC) in multiple stages. Note that the CFO compensation is carried out in time domain by multiplying r_n with $e^{-\frac{j2\pi\epsilon_i n}{N}}$, $i = 1, \cdots, K$ (this method of CFO compensation is referred to as the direct method in [6]). The received signal after CFO compensation and guard time removal for the ith user is given by

$$y_n^{(i)} = r_n e^{-\frac{j2\pi\epsilon_i n}{N}}, \quad 0 \le n \le N-1, \tag{5}$$

which forms the input to the ith DFT block. The output of the DFT block for the ith user on the kth subcarrier is given by

$$Y_k^{(i)} = H_k^{(i)} X_k^{(i)} + \sum_{\substack{l=1 \\ l\neq i}}^{K} \sum_{q\in S_l} \rho_{kq}^{(i),(l)} H_q^{(l)} X_q^{(l)} + Z_k^{(i)}, \tag{6}$$

where

$$\rho_{kq}^{(i),(l)} = \frac{\sin\pi(k-q+\delta_{li})}{N\sin\frac{\pi}{N}(k-q+\delta_{li})} \exp\Big(-j(1-\frac{1}{N})\pi(k-q+\delta_{li})\Big), \tag{7}$$

and δ_{li} is the difference between the ith user and lth user CFO values, given by

$$\delta_{li} = \epsilon_l - \epsilon_i. \tag{8}$$

The channel coefficient $H_k^{(i)}$ is given by (3) and the noise component $Z_k^{(i)}$ is given by

$$Z_k^{(i)} = \sum_{n=0}^{N-1} z_n^{(i)}\, e^{\frac{-j2\pi n(k+\epsilon_i)}{N}}. \tag{9}$$

Note that the 2nd term in (6) represents the MUI present at the DFT output. In the case of single user detection (SUD), the DFT outputs, $Y_k^{(i)}$'s, can be directly used to make the symbol decision. Additional processing (e.g., interference cancellation) may be performed on $Y_k^{(i)}$'s to mitigate the MUI effects.

III. Proposed Weighted Linear PIC Scheme

The proposed multistage weighted linear PIC (WLPIC) scheme is explained as follows. Let m denote the stage index. We take the DFT outputs, $Y_k^{(i)}$'s, in (6) as the first stage ($m = 1$) outputs of the receiver, i.e., $Y_{k,(1)}^{(i)} = Y_k^{(i)}$. In the case of SUD, the symbol decisions are made directly from $Y_{k,(1)}^{(i)}$'s. Parallel interference cancellation is performed in the subsequent stages. In a given PIC stage $m, m > 1$, an estimate of the MUI is made based on the soft values of the previous stage outputs. These MUI estimates are scaled by weights and cancelled from the DFT outputs, $Y_{k,(1)}^{(i)}$.

The interference cancelled output of the ith user on the kth subcarrier in the mth stage, $Y_{k,(m)}^{(i)}$, $m > 1$, can be written as

$$Y_{k,(m)}^{(i)} = Y_{k,(1)}^{(i)} - w_{k,(m)}^{(i)} \underbrace{\sum_{\substack{l=1 \\ l\neq i}}^{K} \sum_{q\in S_l} \rho_{kq}^{(i),(l)} Y_{q,(m-1)}^{(l)}}_{\text{MUI estimate}} \tag{10}$$

where $Y_{k,(1)}^{(i)}$ is the 1st stage output given by (6) and $\rho_{kq}^{(i),(l)}$ is given by (7). It is noted that $\sum_{\substack{l=1 \\ l\neq i}}^{K} \sum_{q\in S_l} \rho_{kq}^{(i),(l)} Y_{q,(m-1)}^{(l)}$ is the MUI estimate, and $w_{k,(m)}^{(i)}$ is the weight with which this MUI estimate is scaled and cancelled. It is noted that the SUD becomes a special case of the proposed WLPIC scheme for

This full text paper was peer reviewed at the direction of IEEE Communications Society subject matter experts for publication in the IEEE ICC 2006 proceedings.

$w^{(i)}_{k,(m)} = 0, \forall i,k,m$. Also, we call the WLPIC scheme with unity weights on all subcarriers (i.e., $w^{(i)}_{k,(m)} = 1, \forall i,k,m$) as conventional LPIC (CLPIC) scheme. In the CLPIC scheme, the operations needed for choice of optimum weights and scaling of MUI estimates with these weights are avoided (because of unity weights). However, performance better than that of the CLPIC can be achieved by using optimum weights. We propose to obtain the optimum weights $w^{(i),opt}_{k,(m)}$ by maximizing the average SIR at the mth stage output.

In an uncoded system, the symbol decision for the ith user on the kth subcarrier at the output of the mth stage can be made based on the output $Y^{(i)}_{k,(m)}$. For example, the symbol decision at the mth stage output for the case of BPSK modulation can be obtained as

$$\widehat{X}^{(i)}_{k,(m)} = \text{sgn}\left(\mathcal{R}e\left(\overline{H^{(i)}_k} Y^{(i)}_{k,(m)}\right)\right), \qquad (11)$$

where $\overline{H^{(i)}_k}$ denotes the conjugate of $H^{(i)}_k$. For the case of M-QAM/M-PSK modulation, symbol decision can be made using the minimum Euclidean distance rule. In a coded system, the $Y^{(i)}_{k,(m)}$'s are fed to the decoder.

IV. Average SIR at 2nd and 3rd Stage Outputs

In [11], we have derived expressions for the average SIR at the output of the 2nd and 3rd stages of the proposed WLPIC scheme. Also, we used these average SIR expressions to obtain closed-form expressions for the optimum weights $w^{(i),opt}_{k,(m)}$. Refer [11] for closed-form expressions for average SIR at 2nd and 3rd stage outputs and the optimum weights.

In Fig. 3, we plot the average SIR at the output of the 2nd stage as a function of weights $w^{(i)}_{k,(2)}$ obtained through both analysis (Eqn. (21) in [11]) as well as simulations. The following system parameters are considered: $N = 32$, $K = 4$, $[\epsilon_1, \epsilon_2, \epsilon_3, \epsilon_4] = [-0.1, 0.3, 0.25, -0.15]$, and SNR=25 dB. The channel model used is a one sample spaced two-ray equal-gain Rayleigh fading model. Two types of subcarrier allocation, namely, a) interleaved allocation and b) block allocation are considered. In block allocation, a consecutive block of subcarriers are alloted to one user, the next block to another user, and so on. In interleaved allocation, the subcarriers of each user are uniformly interleaved with the subcarriers assigned to the other users. The following observations can be made from Fig. 3. For the considered channel model and system parameters, block allocation results in a higher output SIR than interleaved allocation. Also, the maximum average output SIR occurs at an optimum weight (maximum SIR of about 15 dB at $w^{(i)}_{k,(2)} \approx 0.7$ for interleaved allocation and a maximum SIR of about 21 dB at $w^{(i)}_{k,(2)} \approx 0.6$ for block allocation). Closed-form expressions for these optimum weights for 2nd stage and 3rd stage, respectively, are given in Eqns. (32) and (33) in [11].

V. Results and Discussion

In this section, we present the numerical and simulation results of the average SIR and BER performance of the proposed WLPIC scheme and compare with those of other detectors in the recent literature. The channel model used throughout this section is a one sample spaced two-ray equal-gain Rayleigh fading model. In Fig. 4, we plot the analytically computed average SIR as a function of the subcarrier index $k = 1, 2, \cdots, N$ under no noise condition (i.e., $\sigma^2 = 0$) for a) SUD, b) 2nd and 3rd stages of the CLPIC scheme (where $w^{(i)}_{k,(2)} = w^{(i)}_{k,(3)} = 1, \forall i,k$), and c) 2nd and 3rd stages of the WLPIC scheme, for an uplink OFDMA system with $N = 32$ subcarriers, $K = 4$ users, interleaved allocation, and CFOs of the different users $[\epsilon_1, \epsilon_2, \epsilon_3, \epsilon_4] = [-0.1, 0.3, 0.25, -0.15]$.

From Fig. 4, it can be seen that the SUD gives the least SIRs in all subcarriers since no interference cancellation is performed. When interference cancellation is performed using CLPIC scheme (where unity weights are used), the 2nd stage output SIR improves significantly compared to that of SUD. The CLPIC 3rd stage output SIR improves further compared to the CLPIC 2nd stage output SIR. The WLPIC scheme (where optimized weights are used) performs significantly better than both SUD as well as CLPIC. For example, the 3rd stage of the WLPIC results in an average SIR of about 23 dB on all the subcarriers which is significantly larger than those of

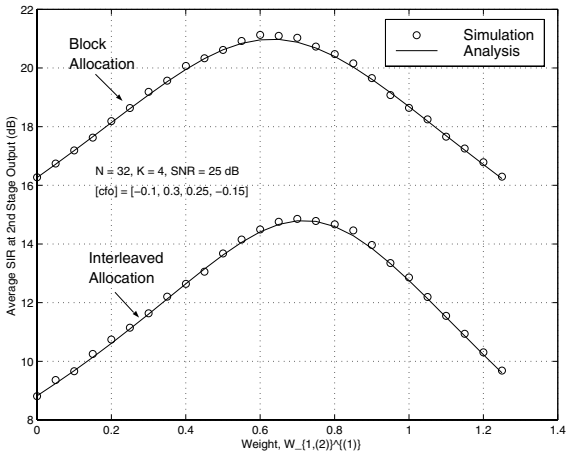

Fig. 3. Average SIR of the 1st user at the 2nd stage output of the proposed WLPIC scheme as a function of the weight on the 1st subcarrier, $w^{(1)}_{1,(2)}$. $N = 32$, $K = 4$, 16-QAM, $[\epsilon_1, \epsilon_2, \epsilon_3, \epsilon_4] = [-0.1, 0.3, 0.25, -0.15]$, SNR = 25 dB. Interleaved and block allocation. Analysis vs simulation.

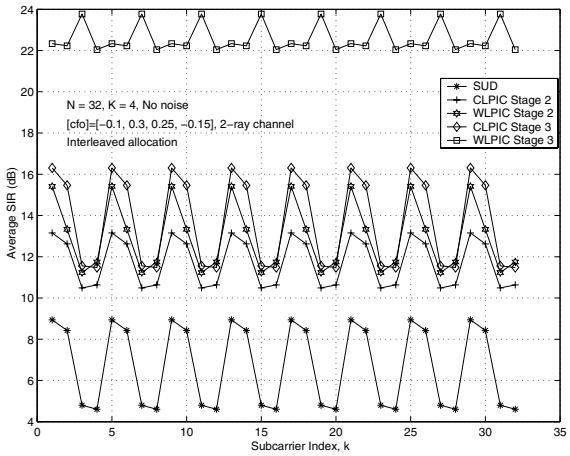

Fig. 4. Average SIR as a function of subcarrier index, k, for different detectors. $N = 32$, $K = 4$, $[\epsilon_1, \epsilon_2, \epsilon_3, \epsilon_4] = [-0.1, 0.3, 0.25, -0.15]$. No noise ($\sigma^2 = 0$). Interleaved allocation. Analysis.

This full text paper was peer reviewed at the direction of IEEE Communications Society subject matter experts for publication in the IEEE ICC 2006 proceedings.

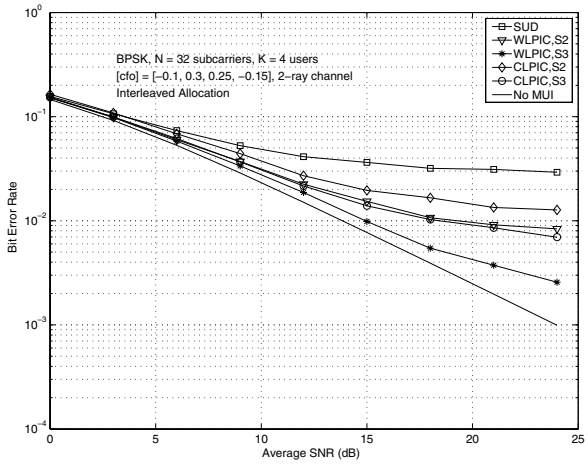

Fig. 5. Bit error rate performance of the proposed WLPIC scheme for BPSK. $N = 32$, $K = 4$, $[\epsilon_1, \epsilon_2, \epsilon_3, \epsilon_4] = [-0.1, 0.3, 0.25, -0.15]$. Interleaved allocation. Simulation.

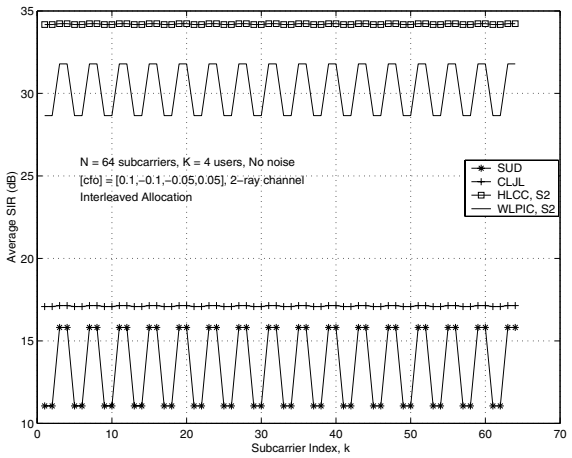

Fig. 6. Comparison of the SIR performance of the proposed WLPIC scheme with HLCC and CLJL schemes. $N = 64$, $K = 4$, $[\epsilon_1, \epsilon_2, \epsilon_3, \epsilon_4] = [\mathbf{0.1}, \mathbf{-0.1}, \mathbf{-0.05}, \mathbf{0.05}]$. No noise ($\sigma^2 = 0$). Interleaved allocation. Analysis.

the other detectors. Thus the performance benefit of using the optimized weights in WLPIC instead of unity weights in CLPIC or zero weights in SUD is clearly evident in Fig. 4.

For the same set of parameters in Fig. 4, we plot the simulated BER performance of SUD, CLPIC (2nd and 3rd stages) and WLPIC (2nd and 3rd stages) in Fig. 5 for BPSK. The single user performance (no MUI) is also shown for comparison purposes. From Fig. 5, it can be seen that the proposed WLPIC scheme results in significantly better BER performance than both the SUD as well as the CLPIC scheme. The 3rd stage of the WLPIC scheme is found to approach the single user (no MUI) performance. We have observed similar SIR and BER improvement for the case of block allocation as well as 16-QAM.

A. Comparison with HLCC and CLJL Schemes

In this subsection, we present a comparison of the performance and complexity of the proposed WLPIC scheme with other detectors reported in the recent literature, namely, a) the HLCC scheme in [9], b) CLJL scheme in [6], and c) SUD. It is noted that while the proposed WLPIC scheme and the HLCC scheme are essentially interference cancellers, the CLJL and SUD schemes are detectors without interference cancellation. Another interesting observation is that while the CLJL and HLCC schemes implement CFO compensation in frequency domain using circular convolution, the SUD and WLPIC schemes implement CFO compensation using the direct time-domain method. Because of this, as we will see next, a HLCC versus WLPIC comparison shows similar comparative behaviour as a CLJL versus SUD comparison, in terms of performance and complexity.

1) SIR and BER Comparison: We note that, since the CFO compensation is done using circular convolution in HLCC scheme, the performance of the HLCC scheme is affected by the individual CFO values of all the users, $\epsilon_i,\ i = 1, 2, \cdots, K$ $\big($see Eqns. (10), (15) and (22) in [9]$\big)$. Whereas in the proposed WLPIC scheme, CFO compensation is done in time domain and hence the performance of the WLPIC scheme is affected by the differences between the desired user's and other users' CFO values, $|\delta_{il}| = |\epsilon_i - \epsilon_l|,\ i, l = 1, 2, \cdots, K$, $i \neq l$ $\big($see Eqns. (6),(7),(8)$\big)$. Because of this, the HLCC scheme performs better than the WLPIC scheme when the individual CFO values are small, whereas the WLPIC scheme performs better than the HLCC scheme when the CFO differences are small. We illustrate both these cases in Figs. 6 through 9, by considering two cases of CFO values, namely, **CFO-1 =** $[\epsilon_1, \epsilon_2, \epsilon_3, \epsilon_4] = [\mathbf{0.1}, \mathbf{-0.1}, \mathbf{-0.05}, \mathbf{0.05}]$, and **CFO-2 =** $[\epsilon_1, \epsilon_2, \epsilon_3, \epsilon_4] = [\mathbf{0.15}, \mathbf{0.12}, \mathbf{0.16}, \mathbf{0.08}]$. It is noted that the CFO-1 values in the above are the same ones used for generating the performance plots in [9]. As can be seen, these CFO-1 values correspond to the case where the individual CFO values are smaller than the difference between the CFO values $\big($e.g., $0.1 < (0.1 - (-0.05)) = 0.15\big)$. On the other hand, CFO-2 values correspond to the case where the CFO differences are smaller than the individual CFO values $\big($e.g., $0.15 > (0.15 - 0.12) = 0.03\big)$.

In Figs. 6 and 7, we present a comparison of the average SIR performance of the various detectors for $N = 64$, $K = 4$, interleaved allocation, and no noise. Figure 6 is for CFO-1 and Fig. 7 is for CFO-2. From Fig. 6, it can be seen that both the HLCC and WLPIC schemes give significantly higher SIR than the CLJL and SUD schemes. Also, HLCC scheme results in higher SIR than WLPIC scheme in this case since the individual CFO values are smaller than the CFO differences. In Fig. 7, on the other hand, we see that the WLPIC scheme offers significantly higher SIR than the HLCC scheme $\big($> 45 dB SIR for WLPIC vs 25 dB SIR for HLCC$\big)$. As pointed out earlier, this is because, though the individual CFO values are large, the CFO differences are smaller for CFO-2. A similar performance behaviour in terms of simulated BER for 16-QAM can be observed in Fig. 8 (for CFO-1) and Fig. 9 (for CFO-2). For similar reasons of CFO implementation in frequency domain versus time domain, it can also be observed that CLJL performs better than SUD for CFO-1 whereas SUD performs better than CLJL for CFO-2. Such scenarios (like CFO-2, where SUD performs better than CLJL) are not discussed in [6] and [9].

Coded FER Performance: We also carried out a comparison study of the various detectors in terms of coded frame error rate (FER) performance. We considered a rate-1/2 convolutional code with constraint length 5. The system parame-

This full text paper was peer reviewed at the direction of IEEE Communications Society subject matter experts for publication in the IEEE ICC 2006 proceedings.

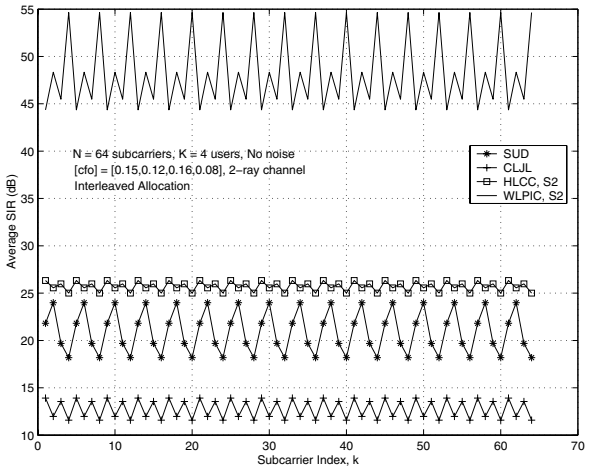

Fig. 7. Comparison of the SIR performance of the proposed WLPIC scheme with HLCC and CLJL schemes. $N = 64$, $K = 4$, $[\epsilon_1, \epsilon_2, \epsilon_3, \epsilon_4] = [\mathbf{0.15}, \mathbf{0.12}, \mathbf{0.16}, \mathbf{0.08}]$. No noise ($\sigma^2 = 0$). Interleaved allocation. Analysis.

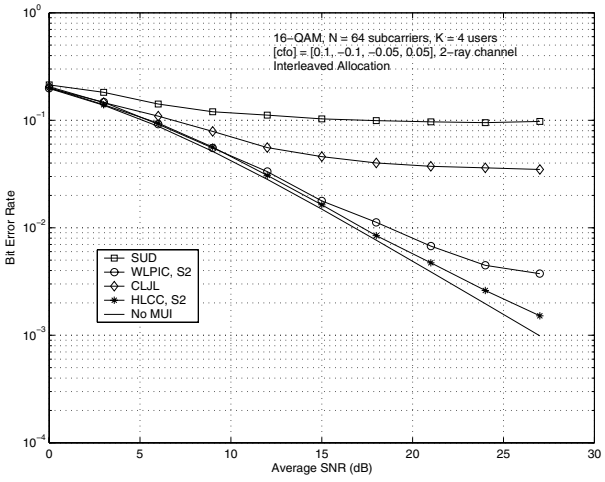

Fig. 8. Bit error rate as a function of average SNR for different detectors for 16-QAM. $K = 4$, $N = 64$, $[\epsilon_1, \epsilon_2, \epsilon_3, \epsilon_4] = [\mathbf{0.1}, \mathbf{-0.1}, \mathbf{-0.05}, \mathbf{0.05}]$. Interleaved allocation. Simulation.

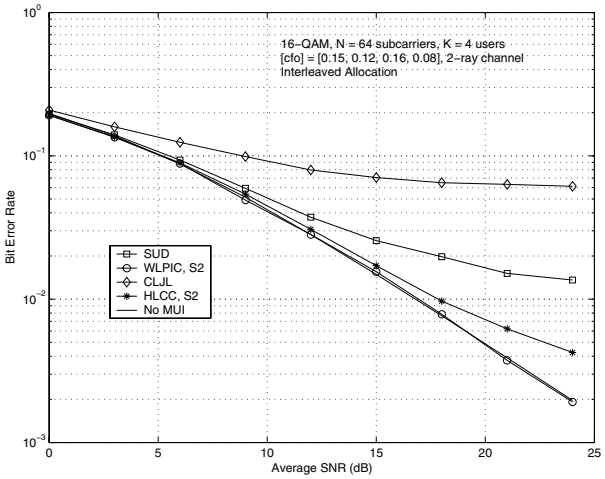

Fig. 9. Bit error rate as a function of average SNR for different detectors for 16-QAM. $K = 4$, $N = 32$, $[\epsilon_1, \epsilon_2, \epsilon_3, \epsilon_4] = [\mathbf{0.15}, \mathbf{0.12}, \mathbf{0.16}, \mathbf{0.08}]$. Interleaved allocation. Simulation.

ters considered include $K = 4$ users, $N = 64$ subcarriers, $[\epsilon_1, \epsilon_2, \epsilon_3, \epsilon_4] = [\mathbf{0.22}, \mathbf{0.2}, \mathbf{0.18}, \mathbf{0.15}]$, interleaved allocation, 4-QAM, and 2-ray Rayleigh fading channel. As in [9], each frame consists of 10 OFDM symbols, and it is assumed that the channels do not vary within one frame but vary from frame to frame. In each frame, an 8×40 block bit interleaver is employed. Figure 10 shows the simulated coded FER performance for various detectors. For this system scenario, WLPIC scheme performs better than HLCC scheme. Again, this is because, in this case, the CFO differences are much smaller than the individual CFO values. Likewise, SUD performs better than CLJL scheme in this scenario.

2) Complexity Comparison: In addition to the above SIR and BER/FER performance comparison, we carried out a complexity comparison among the different detectors as well. The complexities of various detectors in terms of number of complex multiplications required are listed in Table I. The complexities of CLJL and SUD schemes are same as those given in [6]. Compared to CLJL scheme, HLCC has an additional complexity of $N^2 + N^2/K$ per cancellation stage $\big($as per Eqns. (18),(19) in [9]$\big)$. Likewise, compared to SUD scheme, WLPIC has an additional complexity of $N^2 - N^2/K$ per cancellation stage $\big($as per Eqn. (10)$\big)$. The complexity comparison between HLCC and WLPIC schemes as a function of number of subcarriers, N, for $K = 16$ users and $m = 2, 3$ (2nd, 3rd stages) is shown in Fig. 11. It can be seen that for a given K, HLCC is less complex for small N, whereas WLPIC has lesser complexity than HLCC for large N, which is typical in OFDMA systems. For example, for $N = 1024$, $K = 16$ and $m = 2$, HLCC has a complexity of 11,84,768, whereas WLPIC has a lesser complexity of 10,55,232. It is further noted that complexity reduction techniques similar to those given in [9] for HLCC scheme (e.g., by way of ignoring weak subcarriers or other user subcarriers far-off from desired user's subcarriers) can be done for the WLPIC scheme as well. In addition to the performance and complexity comparison presented in the above, effect of imperfect CFO estimation and received power imbalance, as studied for HLCC scheme in [9], can be investigated for the WLPIC scheme also. These effects on WLPIC are expected to be on the same lines as observed for HLCC in [9].

VI. Conclusions

We proposed an interference cancellation scheme for MUI mitigation in uplink OFDMA. The proposed scheme performed CFO compensation in time domain, followed by DFT operations (on a per-user basis) and multistage linear parallel interference cancellation on these DFT outputs. Estimates of the MUI for cancellation were obtained using soft values of the outputs from the previous stages and the MUI estimate were scaled by weights before cancellation. The proposed scheme was shown to effectively cancel the MUI caused by the other user CFOs. We showed that the scheme proposed by Huang and Letaief (HLCC scheme) performs better than our scheme when the individual CFO values are small, whereas our scheme performs better than the HLCC scheme when the CFO differences are small (even if the individual CFO values are large). Also, our scheme has lesser complexity than HLCC scheme when the number of subcarriers is large, which is typical in OFDMA systems.

This full text paper was peer reviewed at the direction of IEEE Communications Society subject matter experts for publication in the IEEE ICC 2006 proceedings.

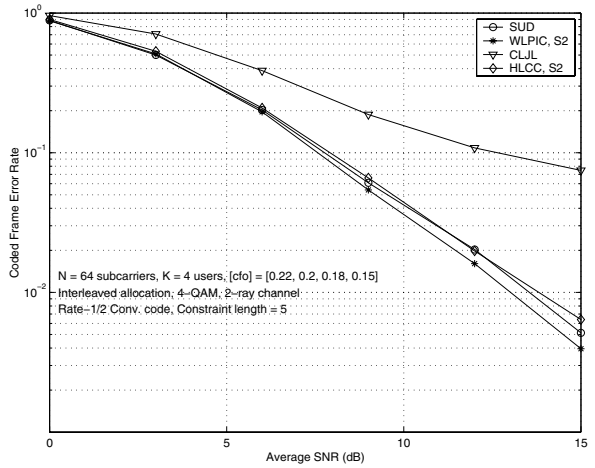

Fig. 10. Coded FER performance comparison among different detectors. $K = 4$, $N = 64$, $[\epsilon_1, \epsilon_2, \epsilon_3, \epsilon_4] = [\mathbf{0.22}, \mathbf{0.2}, \mathbf{0.18}, \mathbf{0.15}]$. Interleaved allocation, 4-QAM, rate-1/2 convolutional code, constraint length = 5. Simulation. WLPIC performs better than HLCC.

Detector	Complexity
CLJL	$\frac{N}{2}\log N + \frac{N^2}{K}$
HLCC	$\frac{N}{2}\log N + \frac{N^2}{K} + (m-1)\left[N^2 + \frac{N^2}{K}\right]$
SUD	$\frac{KN}{2}\log N - \left[\frac{KN}{2}\log K - \frac{3}{2}(K-1)N\right]$
WLPIC	$\frac{KN}{2}\log N - \left[\frac{KN}{2}\log K - \frac{3}{2}(K-1)N\right]$ $+ (m-1)\left[N^2 - \frac{N^2}{K}\right]$

TABLE I – Complexity comparison among different detectors.

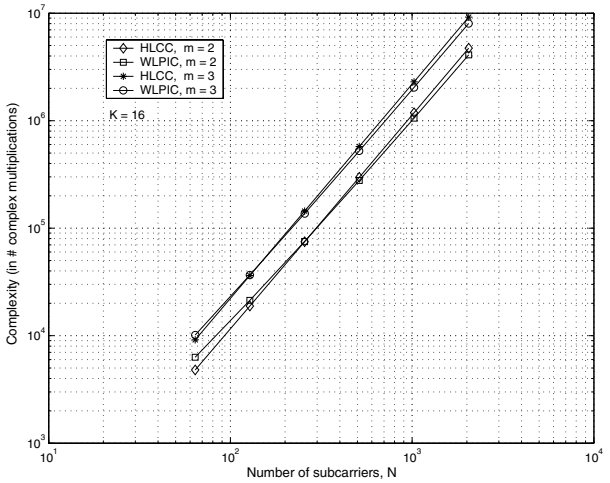

Fig. 11. Complexity comparison of the proposed WLPIC scheme with HLCC scheme. $K = 16$, $m = 2, 3$.

REFERENCES

[1] K. Kim, Y. Han, and S-L. Kim, "Joint subcarrier and power allocation in uplink OFDMA systems," *IEEE Comm. Letters,* vol. 9, no. 6, pp. 526-528, June 2005.

[2] Z. R. Cao, U. Tureli, and Y-D. Yao, "Deterministic multiuser carrier frequency offset estimation for interleaved OFDMA uplink," *IEEE Trans. on Commun.,* vol. 52, no. 9, pp. 1585-1594, 2004.

[3] H. Wang and B. Chen, "Asymptotic distributions and peak power analysis for uplink OFDMA," *Proc. IEEE ICASSP'2004*, May 2004.

[4] M. O. Pun, C.-C. J. Juo, and M. Morelli, "Joint synchronization and channel estimation in uplink OFDMA systems," *Proc. IEEE ICASSP'2005*, March 2005.

[5] A. M. Tonello, N. Laurenti, and S. Pupolin, "Analysis of the uplink of an asynchronous multiuser DMT OFDMA system impaired by time offsets, frequency offsets, and multipath fading," *Proc. IEEE VTC'2000 (Fall)*, vol. 3, pp. 1094-1099, October 2000.

[6] J. Choi, C. Lee, H. W. Jung, and Y. H. Lee, "Carrier frequency offset compensation for uplink of OFDM-FDMA systems," *IEEE Commun. Letters*, vol. 4, no. 12, pp. 414-416, December 2000.

[7] Z. Cao, U. Tureh, and Y. D. Yao, "Analysis of two receiver schemes for interleaved OFDMA uplink signals," *36th Asilomar Conf. on Signals, Systems and Computers,* vol. 2, pp.1818-1821, November 2002.

[8] R. Fantacci, D. Marabissi, and S. Papini, "Multiuser interference cancellation receivers for OFDMA uplink communications with carrier frequency offset," *Proc. IEEE GLOBECOM'04*, pp. 2808-2812, 2004.

[9] D. Huang and K. B. Letaief, "An interference cancellation scheme for carrier frequency offsets correction in OFDMA systems," *IEEE Trans. on Commun.,* vol. 53, no. 7, pp. 1155-1165, July 2005.

[10] D. Sreedhar and A. Chockalingam, "MMSE receiver for multiuser interference cancellation in uplink OFDMA," *Proc. IEEE VTC'2006 (Spring)*, Melbourne, May 2006.

[11] S. Manohar, V. Tikiya, D. Sreedhar, and A. Chockalingam, "A multiuser interference cancellation scheme for uplink OFDMA," *Proc. IEEE WCNC'2006*, April 2006.

This full text paper was peer reviewed at the direction of IEEE Communications Society subject matter experts for publication in the IEEE ICC 2006 proceedings.